

On the acidity of cyclopropanaphthalenes Gas phase and computational studies

Ivana Antol^a, Zoran Glasovac^a, Michael C. Hare^{b,1},
Mirjana Eckert-Maksic^{a,2}, Steven R. Kass^{b,*}

^a Division of Organic Chemistry and Biochemistry, Rudjer Boskovic Institute, P.O. Box 180, HR-10002 Zagreb, Croatia

^b Department of Chemistry, University of Minnesota, Minneapolis, MN 55455, USA

Received 16 January 2002; accepted 9 July 2002

Dedicated to Jesse Beauchamp on the occasion of his 60th birthday.

Abstract

1*H*-Cyclopropa[b]naphthalene (**3H**) and 2-methylnaphthalene (**6H**) were deprotonated by fluoride ion in a Fourier transform mass spectrometer, and their acidities were measured via equilibrium techniques ($\Delta G_{\text{acid}}^{\circ} = 357.5 \pm 2.1 \text{ kcal mol}^{-1}$ (**3H**) and $365.2 \pm 2.1 \text{ kcal mol}^{-1}$ (**6H**), $\Delta H_{\text{acid}}^{\circ} = 365.1 \pm 2.1 \text{ kcal mol}^{-1}$ (**3H**) and $372.7 \pm 2.1 \text{ kcal mol}^{-1}$ (**6H**)). These results were modeled by MP2 and BVWN5 calculations, and additional computations were carried out on benzocyclopropene (**1H**), toluene (**2H**), 1*H*-cyclopropa[a]naphthalene (**4H**), and 1-methylnaphthalene (**5H**). The stability of the conjugate bases of **3H** and **4H** are examined and their aromatic vs. antiaromatic nature is considered. (Int J Mass Spectrom 222 (2003) 11–26)
© 2002 Elsevier Science B.V. All rights reserved.

Keywords: Aromaticity; Antiaromaticity; Cycloproparenes; FTMS; Ab initio; DFT calculations

1. Introduction

Cycloproparenyl anions have aroused considerable interest in organic synthesis since the formation of the parent cyclopropabenzyl anion (**1**) was reported by Eaborn et al. [1]. Current efforts in this area have focused on the preparation of highly strained alkylidenecycloproparenes [2,3], some of which exhibit exceptional fluorescent characteristics [4]. Recently, anion **1** was generated in the gas phase by depro-

tonation of its conjugate acid **1H** [5,6] enabling the intrinsic thermodynamic properties and gas phase reactivity of this fascinating species to be probed in the absence of complicating ion-pairing, solvation and aggregation effects. Two important conclusions emerged from this study. First, it was shown that fusion of a benzene ring on to cyclopropene enhances the acidity of the methylenic position of the three-membered ring by $34.5 \text{ kcal mol}^{-1}$ [1 cal = 4.184 J]. Second, it was found that in the gas phase the conjugate acid of **1** is slightly less acidic than toluene (**2H**), which contrasts with their acidity ordering in condensed media [7].

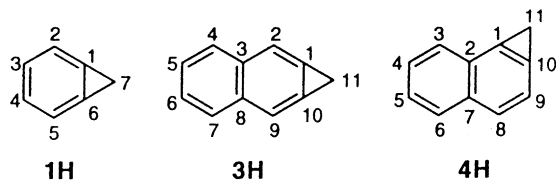
The present study focuses on the determination of the gas phase acidities of cyclopropanaphthalenes **3H**

* Corresponding author. E-mails: mmaksic@emma.irb.hr, kass@chem.umn.edu

¹ Present address: Department of Chemistry, Ohio University, Athens, OH 45701, USA.

² Co-corresponding author.

and **4H** by experimental and computational methods. These species



were examined for several reasons. First, differences in reactivity between the linear (**3H**) and angular (**4H**) isomers resulting from bond localization properties of the naphthalene moiety [8] make them challenging model compounds from a theoretical point of view; both of these hydrocarbons have been described in the literature [9], but only **3H** can be isolated and is stable at room temperature [9,10]. Second, it is of interest to assess the extent of any antiaromatic destabilization [11] in the corresponding anions and compare it with that found in **1** [5]. Third, the accurate determination of intrinsic thermodynamic properties of these species along with reliable calculations of their structural features are expected to provide an important supplement to understanding the chemistry of cyclopropanes in solution, and the role of solvents in affecting their reactivity under basic conditions. For comparison sake we also carried out calculations on 1-methylnaphthalene (**5H**) [12] and 2-methylnaphthalene (**6H**) and measured the acidity of the latter compound.

2. Experimental

Cyclopropanaphthalene **3H** was synthesized according to the published procedure of Halton and coworkers [9]. 2-Methylnaphthalene and all of the reference acids employed in this work were commercially available and used as supplied.

Gas phase experiments were carried out with a dual cell model 2001 Finnigan Fourier transform mass spectrometer (FTMS) equipped with a 3.0 T superconducting magnet and operated by a Sun workstation running the Odyssey software package. In this work the acids of interest were deprotonated by fluoride ion,

which was generated by electron ionization of carbon tetrafluoride. The resulting M-1 ions were isolated using a combination of chirp excitations and SWIFT waveforms [13,14]. They were then transferred to the second cell of the instrument and vibrationally cooled with a pulse of argon. Neutral reagents were added via slow-leak valves and every reaction was monitored as a function of time. Equilibrium constants were determined by measuring the forward and reverse rate constants ($K = k_f/k_r$) for proton transfer reactions with standard reference acids at 300 K [15]. Aniline and *p*-fluoroaniline were used in the case of **3H**, while allyl and neopentyl alcohol were utilized with 2-methylnaphthalene.

Ab initio and density functional theory (DFT) calculations were carried out using Gaussian 94 [16], Gaussian 98 [17], and GAMES-US [18] on Unix-based workstations or Linux-based Pentium III PC's at the University of Minnesota, Minnesota Supercomputer Institute, and Rudjer Boskovic Institute. Full geometry optimizations in a given point group were first attempted at the MP2 level of theory using the frozen core (FC) approximation [19] and the 6-31+G(d) basis set [20]. This method provides good results in describing subtle changes in molecular structure induced by the fusion of a small strained ring in cycloalkarenes [21], and gives accurate acidities of structurally related species as indicated in our previous studies [5,22]. In this work, surprisingly, we were unable to converge some of the anion structures. Therefore, we optimized all of the species of interest with the 6-31G(d) basis set and also carried out BVWN5/6-31+G(d) optimizations [23]. Vibrational analyses at both levels of theory were performed to verify the nature of each computed structure and to obtain thermochemical data (zero-point energies and temperature corrections). All of the computed geometries were found to be minima on the potential energy surface except for the MP2/6-31G(d) planar anions **3pl** (C_{2v}) and **4pl** (C_s), which turned out to be second-order saddle points with two imaginary frequencies ($300.6i$ and $530.3i$ cm^{-1} (**3pl**) and $324.7i$ and $777.3i$ cm^{-1} (**4pl**)).

Deprotonation energies (Table 1) were calculated at the MP2/6-31+G(d)//MP2/6-31G(d) and BVWN5/

Table 1
 Calculated electronic energies, zero-point energies, and acidities for **1H–6H**

Compound	Energy		$\Delta H_{\text{acid}}^{\circ}$ ^a	Energy		$\Delta H_{\text{acid}}^{\circ}$ ^a	Experiment
	MP2	ZPE		DFT	ZPE		
1H	–269.36858 (–269.25997)	0.10215		–271.62161 (–271.51336)	0.10201		
1	–268.74009 (–268.64741)	0.08594	385.9 [385.7] ^b	–270.99080 (–270.90272)	0.08572	387.2	386 ± 3 ^b
2H	–270.64413 (–270.51225)	0.12471		–272.96669 (–272.83475)	0.12513		
2	–270.01819 (–269.90285)	0.10761	383.9 [384.3] ^b	–272.34015 (–272.22410)	0.10906	384.7	382.3 ± 0.3 ^c
3H	–422.53460 (–422.37936)	0.14591		–426.00934 (–425.85271)	0.14767		
3	–421.93136 (–421.79444)	0.13056	368.5	–425.40525 (–425.26457)	0.13152	370.5	365.1 ± 2.1
3pl	–421.93450 (–421.79316)	0.12824	369.3	–425.40349 (–425.26352)	0.13064	371.2	
4H	–422.53520 (–422.37963)	0.14641		–426.00798 (–425.85178)	0.14769		
4	–421.90682 (–421.76736)	0.12990	385.7	–425.37940 (–425.23962)	0.13099	385.6	
4pl	–421.89392 (–421.75673)	0.12693	392.4	–425.37029 (–425.23160)	0.12957	390.6	
5H	–423.80976 (–423.63050)	0.16939		–427.35103 (–427.17045)	0.17155		374.1 ± 2.1 ^d ,
5	–423.19792 (–423.03351)	0.15477	376.1	–426.73795 (–426.57346)	0.15542	376.1	370.7 ± 2.5 ^e
6H	–423.81003 (–423.63123)	0.16882		–427.35335 (–427.17273)	0.17109		
6	–423.19793 (–423.03379)	0.15434	376.4	–426.74096 (–426.57614)	0.15517	375.8	372.7 ± 2.1

MP2, DFT, and ZPE energies in a.u. Acidities in kilocalories per mole. MP2 = MP2/6-31+G(d)//MP2/6-31G(d) and DFT = BVWN5/6-31+G(d). MP2/6-31G(d) ZPEs are scaled by 0.9670 while the vibrational frequencies used for correcting the temperature from 0 to 298 K are scaled by 0.9427 [24]. Parenthetical energies have been corrected to 298 K and include an RT work term.

^a Acidities are at 298 K. Values in brackets correspond to MP2/6-31+G(d)//MP2/6-31+G(d) acidities.

^b [5].

^c [42].

^d [12a].

^e [12b].

Table 2
MP2/6-31G(d) and BVWN5/6-31+G(d) geometries for **3H**, **3**, **3pl**, **4H**, **4**, and **4pl**

Bond	3H	3	3pl	Bond	4H	4	4pl
C1–C2	1.365 (1.373)	1.364 (1.376)	1.363 (1.376)	C1–C2	1.402 (1.414)	1.397 (1.407)	1.400 (1.412)
C2–C3	1.433 (1.451)	1.457 (1.473)	1.462 (1.478)	C2–C3	1.415 (1.430)	1.423 (1.436)	1.418 (1.429)
C3–C4	1.419 (1.431)	1.407 (1.419)	1.405 (1.416)	C3–C4	1.381 (1.391)	1.377 (1.389)	1.377 (1.393)
C4–C5	1.379 (1.392)	1.399 (1.415)	1.402 (1.419)	C4–C5	1.414 (1.428)	1.430 (1.447)	1.437 (1.453)
C5–C6	1.412 (1.424)	1.396 (1.408)	1.393 (1.404)	C5–C6	1.381 (1.391)	1.377 (1.386)	1.371 (1.382)
C3–C8	1.449 (1.465)	1.446 (1.465)	1.446 (1.466)	C6–C7	1.419 (1.433)	1.429 (1.446)	1.443 (1.457)
C1–C10	1.367 (1.379)	1.417 (1.432)	1.433 (1.448)	C7–C8	1.433 (1.444)	1.402 (1.411)	1.387 (1.397)
C1–C11	1.500 (1.518)	1.420 (1.434)	1.397 (1.408)	C8–C9	1.390 (1.403)	1.429 (1.448)	1.461 (1.479)
Angle				C9–C10	1.400 (1.411)	1.384 (1.392)	1.365 (1.377)
C10–C11–C1	54.2 (54.2)	59.9 (59.9)	61.7 (61.9)	C1–C10	1.338 (1.344)	1.373 (1.385)	1.405 (1.419)
C10–C1–C11	62.9 (62.9)	60.1 (60.0)	59.1 (59.0)	C2–C7	1.447 (1.466)	1.474 (1.498)	1.485 (1.512)
C10–C1–C2	125.0 (124.8)	123.5 (123.3)	123.6 (123.3)	C1–C11	1.507 (1.522)	1.456 (1.473)	1.383 (1.397)
C1–C2–C3	113.8 (114.5)	115.5 (116.4)	115.6 (116.4)	C10–C11	1.506 (1.522)	1.486 (1.503)	1.449 (1.455)
C2–C3–C8	121.2 (120.7)	120.5 (120.1)	120.8 (120.3)	Angle			
C8–C3–C4	118.4 (118.3)	118.0 (118.0)	118.0 (118.0)	C10–C11–C1	52.7 (52.4)	55.6 (55.5)	59.4 (59.6)
C3–C4–C5	121.4 (121.5)	122.6 (122.5)	122.7 (122.6)	C10–C1–C11	63.6 (63.8)	63.3 (63.4)	62.6 (62.2)
C4–C5–C6	120.2 (120.1)	119.4 (119.4)	119.3 (119.4)	C11–C10–C1	63.6 (63.8)	61.1 (61.2)	57.9 (58.1)
α^a	56.7 (56.5)	35.0 (36.7)		C10–C1–C2	125.1 (125.2)	123.5 (123.8)	123.5 (123.7)
				C1–C2–C7	112.0 (112.4)	114.2 (114.3)	113.3 (113.7)
				C7–C2–C3	120.2 (119.8)	119.2 (119.0)	120.3 (119.9)
				C2–C3–C4	119.9 (120.3)	121.4 (121.7)	121.8 (122.0)
				C3–C4–C5	120.5 (120.5)	119.7 (119.6)	118.7 (118.7)
				C4–C5–C6	120.7 (120.6)	120.7 (120.8)	121.4 (121.5)
				C5–C6–C7	120.9 (121.2)	122.0 (122.2)	122.5 (122.5)
				C6–C7–C2	117.8 (117.7)	116.7 (116.6)	115.1 (115.2)
				C2–C7–C8	121.4 (120.9)	120.7 (120.2)	121.9 (121.1)
				C7–C8–C9	123.1 (123.1)	121.9 (122.2)	122.1 (122.4)
				C8–C9–C10	113.2 (113.6)	115.4 (115.6)	114.8 (115.1)
				C9–C10–C1	125.0 (124.8)	123.6 (123.5)	124.3 (124.0)
				α	56.5 (56.4)	53.3 (53.6)	

All distances are in angstroms and angles in degrees. Parenthetical values correspond to the DFT results.

^a Out-of-plane angle of the hydrogen attached to C11.

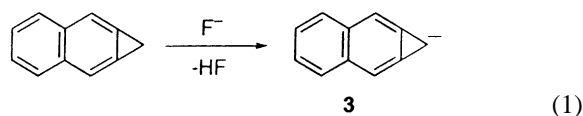
6-31+G(d) levels (abbreviated hereafter as MP2 and DFT, respectively) and are corrected for the corresponding ZPEs energies scaled by factors of 0.9670 (MP2) [24] and 1.00 (DFT). To obtain the energies at 298 K, the MP2 and DFT harmonic frequencies used in calculating the temperature corrections were scaled by 0.9427 [24] and 1.00, respectively. Radicals were computed using the UBVWN5/6-31+G(d) method, and the spin contamination of the wave function was found to be acceptable (i.e., $\langle s^2 \rangle < 0.78$). Subsequently, bond dissociation energies and electron affinities were computed at 298 and 0 K, respectively.

The key structural parameters calculated for **3H**, **4H**, and their anions (**3**, **3pl**, **4**, and **4pl**) are summarized in Table 2. Bond distances and bond angles for **5H**, **6H**, and their anions (**5** and **6**) are given in Appendix A. Bonding characteristics of some of these species were investigated using simple qualitative bond indices such as hybridization [25] and Coulson's π -bond orders of the mobile π -electrons [26]. The reported *s*-characters were calculated at the MP2/6-31G(d) level via the natural bond orbital (NBO) analysis method of Reed and coworkers [27] as implemented in the Gaussian 94 package [28]. Atomic charges, π -electron densities and π -bond orders were derived for the MP2 optimized structures using a density partitioning scheme based upon symmetric Löwdin orthogonalization [29]. A topological analysis of the electron density and its Laplacian also was carried out using the atoms in molecules (AIM) theory of Bader [30] on MP2 wave functions for the MP2/6-31G(d) optimized structures of **3H**, **4H**, and their corresponding anions.

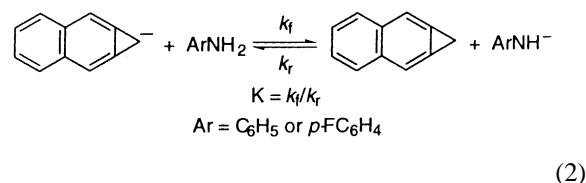
3. Results and discussion

3.1. Acidity determinations

Cyclopropanaphthalene **3H** was deprotonated in the gas phase by fluoride ion Eq. (1) and as expected,



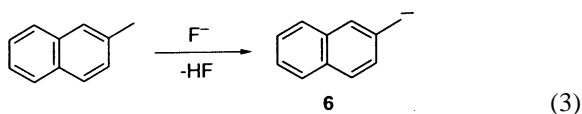
the conjugate base undergoes one exchange of hydrogen by deuterium upon reaction with *tert*-BuOD. To establish the proton affinity of **3** (or equivalently $\Delta H_{\text{acid}}^\circ(\mathbf{3H})$), equilibrium constants with aniline and *p*-fluoroaniline were determined by measuring rate constants for the forward (k_f) and reverse (k_r) proton transfer reactions Eq. (2). When aniline is the reference acid,



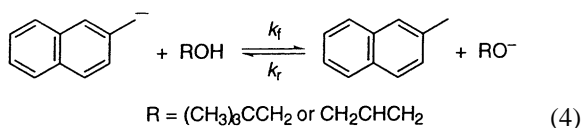
$k_f = 4.10 \pm 0.29 \times 10^{-10} \text{ cm}^3 \text{ molecule}^{-1} \text{ s}^{-1}$ (4) and $k_r = 4.85 \pm 0.05 \times 10^{-9} \text{ cm}^3 \text{ molecule}^{-1} \text{ s}^{-1}$ (2), where the numbers in parentheses correspond to the number of independent measurements that were carried out and the cited uncertainty represents the standard deviation in the data. The resulting equilibrium constant is 0.0845 ± 0.0060 , but a more conservative error of $\pm 100\%$ is adopted for the rest of the data analysis because of the difficulties in measuring neutral reagent pressures with an ion gauge. This leads to $\Delta G_{\text{acid}}^\circ(\text{aniline}) - \Delta G_{\text{acid}}^\circ(\mathbf{3H}) = 1.47 \pm 0.59 \text{ kcal mol}^{-1}$, which can be combined with the known $\Delta G_{\text{acid}}^\circ(\text{aniline}) = 359.1 \pm 2.0 \text{ kcal mol}^{-1}$ [31,32] and a calculated $\Delta S_{\text{acid}}^\circ(\mathbf{3H}) = 25.3 \text{ e.u.}$ using HF/6-31+G(d) geometries and vibrational frequencies to obtain $\Delta G_{\text{acid}}^\circ(\mathbf{3H}) = 357.6 \pm 2.1 \text{ kcal mol}^{-1}$ and $\Delta H_{\text{acid}}^\circ(\mathbf{3H}) = 365.2 \pm 2.1 \text{ kcal mol}^{-1}$. In a similar manner, $k_f = 2.02 \pm 0.088 \times 10^{-9} \text{ cm}^3 \text{ molecule}^{-1} \text{ s}^{-1}$ (3) and $k_r = 1.32 \pm 0.40 \times 10^{-9} \text{ cm}^3 \text{ molecule}^{-1} \text{ s}^{-1}$ (5) when *p*-fluoroaniline is used as the reference acid. This leads to $\Delta \Delta G_{\text{acid}}^\circ = -0.25 \pm 0.60 \text{ kcal mol}^{-1}$, which can be combined with $\Delta G_{\text{acid}}^\circ(p\text{-FC}_6\text{H}_4\text{NH}_2) = 357.0 \pm 2.0 \text{ kcal mol}^{-1}$ to obtain $\Delta G_{\text{acid}}^\circ(\mathbf{3H}) = 357.3 \pm 2.1 \text{ kcal mol}^{-1}$ and $\Delta H_{\text{acid}}^\circ(\mathbf{3H}) = 364.9 \pm 2.1 \text{ kcal mol}^{-1}$. Both acidity measurements are in excellent accord with each other and their average provides our final values: $\Delta G_{\text{acid}}^\circ(\mathbf{3H}) = 357.5 \pm 2.1 \text{ kcal mol}^{-1}$ and $\Delta H_{\text{acid}}^\circ(\mathbf{3H}) = 365.1 \pm 2.1 \text{ kcal mol}^{-1}$. Attempts to measure the acidity of

4H, unfortunately, were unsuccessful as this compound is known to be quite labile [8,9], and we were unable to successfully prepare and purify it.

For comparison purposes, 2-methylnaphthalene (**6H**) also was examined. Fluoride ion readily deprotonates this aromatic hydrocarbon to afford the “benzylic” anion **6** Eq. (3), and as expected for this structure,



the conjugate base undergoes 2 hydrogen-deuterium exchanges upon reaction with *tert*-BuOD. Equilibrium constants were measured with neopentyl alcohol and allyl alcohol to determine the acidity of **6H** as was done for cyclopropanaphthalene Eq. (4). In the former case,



$k_f = 4.58 \pm 0.65 \times 10^{-10} \text{ cm}^3 \text{ molecule}^{-1} \text{ s}^{-1}$ (4) and $k_r = 2.43 \pm 0.61 \times 10^{-9} \text{ cm}^3 \text{ molecule}^{-1} \text{ s}^{-1}$ (4), which leads to $K = 0.188 \pm 0.054$ and $\Delta\Delta G_{\text{acid}}^\circ = 1.00 \pm 0.60 \text{ kcal mol}^{-1}$. Given that $\Delta G_{\text{acid}}^\circ$ (neopentyl alcohol) = $366.0 \pm 2.0 \text{ kcal mol}^{-1}$ and our calculated $\Delta S_{\text{acid}}^\circ$ (**6H**) = 25.1 e.u. using HF/6-31G(d) geometries and harmonic frequencies, we obtain $\Delta G_{\text{acid}}^\circ$ (**6H**) = $365.0 \pm 2.1 \text{ kcal mol}^{-1}$ and $\Delta H_{\text{acid}}^\circ$ (**6H**) = $372.5 \pm 2.1 \text{ kcal mol}^{-1}$. In the latter instance, $k_f = 3.28 \pm 0.33 \times 10^{-10} \text{ cm}^3 \text{ molecule}^{-1} \text{ s}^{-1}$ (2), $k_r = 2.04 \pm 0.35 \times 10^{-9} \text{ cm}^3 \text{ molecule}^{-1} \text{ s}^{-1}$ (4), $K = 0.161 \pm 0.032$, and $\Delta\Delta G_{\text{acid}}^\circ = 1.09 \pm 0.60 \text{ kcal mol}^{-1}$. Given that $\Delta G_{\text{acid}}^\circ$ (allyl alcohol) = $366.6 \pm 2.8 \text{ kcal mol}^{-1}$, these results lead to $\Delta G_{\text{acid}}^\circ$ (**6H**) = $365.5 \pm 2.9 \text{ kcal mol}^{-1}$ and $\Delta H_{\text{acid}}^\circ$ (**6H**) = $373.0 \pm 2.9 \text{ kcal mol}^{-1}$. So our final values are $\Delta G_{\text{acid}}^\circ$ (**6H**) = $365.2 \pm 2.1 \text{ kcal mol}^{-1}$ and $\Delta H_{\text{acid}}^\circ$ (**6H**) = $372.7 \pm 2.1 \text{ kcal mol}^{-1}$.

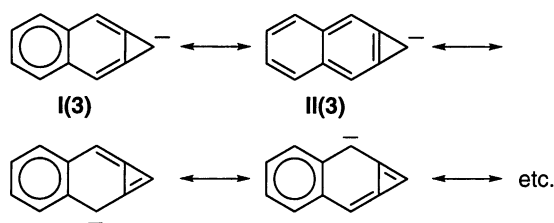
The results of acidity calculations for isomeric cyclopropanaphthalenes **3H** and **4H** are given in Table 1

along with their acyclic reference compounds, 1-methylnaphthalene (**5H**) and 2-methylnaphthalene (**6H**). Also included for comparison purposes are MP2/6-31+G(d)//MP2/6-31G(d), and MP2/6-31+G(d) results from our previous study on benzocyclopropene and toluene [5]. In each case only deprotonation at the benzylic center is considered. Our results indicate the MP2/6-31+G(d)//MP2/6-31G(d) acidities of **1H** and **2H** differ from those in which diffuse functions are included in the geometry optimization by less than 1 kcal mol^{-1} [33]. This suggests that both computational approaches are equally reliable for the species of interest in this work.

Both the MP2 and DFT acidities of **1H–6H** agree with each other to within 2 kcal mol^{-1} and are in reasonable accord with experiment, but are consistently bigger than the experimental values. The largest discrepancies are for **3H** ($3.4 \text{ kcal mol}^{-1}$ for MP2 and $5.4 \text{ kcal mol}^{-1}$ for DFT) and **6H** ($3.7 \text{ kcal mol}^{-1}$ for MP2 and $3.1 \text{ kcal mol}^{-1}$ for DFT), but their difference ($7.6 \pm 3.0 \text{ kcal mol}^{-1}$) is well reproduced at the MP2 ($7.9 \text{ kcal mol}^{-1}$) and DFT ($5.3 \text{ kcal mol}^{-1}$) levels. Unfortunately, a comparison cannot be made with the experimental acidity for **4H** since, as mentioned above, we have not succeeded in preparing this compound. Nevertheless, it appears that the acidity is close to that of **1H** and is approximately 10 kcal mol^{-1} less than that of 1-methylnaphthalene or 2-methylnaphthalene.

3.2. Energetic, structural and electronic features of the cyclopropanaphthalenyl anions

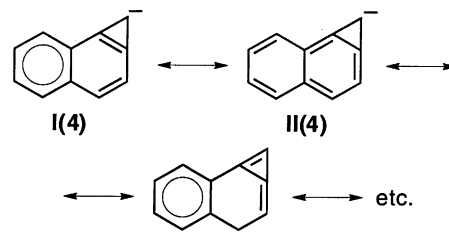
Linear (**3H**) and angular (**4H**) cyclopropanaphthalenes differ in energy by less than 1 kcal mol^{-1} at the MP2 and DFT levels yet their acidities are predicted to be different by 16 kcal mol^{-1} ($17.2 \text{ kcal mol}^{-1}$ for MP2 and $15.1 \text{ kcal mol}^{-1}$ for DFT). Clearly, this is due to the difference in the stabilities of their conjugate bases. This raises the question, why is **3** so much more stable than **4**? This can be answered qualitatively by considering the resonance structures of the anions. First, let us focus on the most relevant resonance structures of the linear isomer (Scheme 1). The π -electron coupling schemes denoted by **I(3)**



Scheme 1.

and **II(3)** we shall term the principal or cardinal resonance structures because they correspond to electron confinement at the deprotonation center, and the location with the largest amount of charge. They are not, however, of the same importance. Structure **I(3)** is energetically more favorable than **II(3)** for several reasons. First, it involves a formed sextet within the peripheral benzene moiety, which should be advantageous according to Clar's rule [34]. Further, the double bonds emanating from the cyclopropenyl ring are positioned in the best way to avoid the lone pair of the anionic center and thereby minimize any antiaromatic interaction [35,36]. Finally, the π -bond localization pattern is compatible with rehybridization at the carbon junction atoms predicted by the Mills–Nixon effect [37,38]. In contrast, resonance structure **II(3)** implicitly suffers from a strong antiaromatic interaction in the three-membered ring and the antagonistic distribution of the π -electron density and *s*-characters in the annelated (C1–C10) and *ortho* (C1–C2 and C9–C10) carbon–carbon bonds of the aromatic ring. The latter resonance structure, consequently, has a low weight associated with it and can be disregarded in the qualitative discussion of the spatial and electronic structure of **3**. Of the 12 remaining resonance structures for **3**, we present only two in Scheme 1 because they both include an aromatic sextet and provide along with **I(3)** a good basis for rationalizing the gross geometric features of **3**.

The π -bonding pattern in **4** described by the resonance structures depicted in Scheme 2 is markedly different than for **3**. The structure **I(4)** embodies a strong antiaromatic interaction and to a first approximation it can be omitted from the forthcoming discussion. Consequently, only one cardinal structure should be re-



Scheme 2.

tained (**II(4)**), and it does not have a benzenoid peripheral ring but rather the qualitative localized π -electron pattern of *cis*-1,3-butadiene. Hence, one concludes on intuitive grounds that **4** should be less stable than **3**. This conclusion is corroborated by both MP2 and BVWN5 calculations which indicate that at 298 K the latter ion is favored by 17.2 kcal mol⁻¹ (MP2) and 15.1 kcal mol⁻¹ (DFT).

The resonance structures depicted in Schemes 1 and 2 also are very useful in rationalizing the gross structural changes of **3H** and **4H** induced by deprotonation. Not surprisingly, the three-membered ring which contains the deprotonation site undergoes the largest change. Ion **3** is not planar but is pyramidal and has a C11–H out-of-plane angle (α) of 35° at the MP2 level; in the following discussion MP2 results are given unless otherwise stated. As a result, the lone pair of electrons is not perpendicular to the carbon framework presumably, so as to minimize any antiaromatic interaction within the three-membered ring. Delocalization of the charge over the C1–C11 and C10–C11 bonds takes place nevertheless, and results in a substantial (0.08 Å) shortening of their interatomic distances relative to **3H**. As for the annelated bond, it is elongated by 0.05 Å. This leads to practically an equilateral three-membered ring both at the MP2 and DFT levels. Another noteworthy feature related to the carbon junction atoms is the large C2–C1–C11 angle of 176.2° in **3**, which means that the C1–C2 and C1–C11 bonds are almost colinear. As a result, the electron density distributions at C1 and C10 are severely deformed and this leads to increased angular strain in the three-membered ring. Other changes in the carbon–carbon bond lengths are not as dramatic and can be inferred from the principal resonance structure

I(3). That is, the C2–C3 bond is lengthened, and the C–C bonds within the peripheral benzene ring equalize and become closer to the value for free benzene.

In angular anion **4** the picture is somewhat more complicated because the ion has C_1 symmetry, but the geometric changes are similar to those for **3**. For example, the C1–C10 bond lengthens by 0.035 Å upon deprotonation of **4H**, but this change is less than in the linear species since the small ring is fused to a bond possessing higher π -electron density and therefore is more difficult to stretch. Both apical bonds (C1–C11 and C10–C11) shorten but in an asymmetrical way (0.051 and 0.020 Å, respectively), which is consistent with the resonance structures presented in Scheme 2. That is, there is one more structure describing π -bond localization into the C1–C11 bond than the C10–C11 bond. As a consequence, the cyclopropenyl ring has three nonequivalent C–C bonds all of which have different bond lengths. If resonance structure **II(4)** is dominant as we suggested, and Clar's rule does not hold due to an unfavorable antiaromatic interaction in **I(4)**, then the remaining C–C bond distances of the naphthalene moiety should exhibit changes compatible with its π -electron localization pattern. This conjecture is corroborated by the MP2 and DFT calculations summarized in Table 3, and leads to significant bond alternation in the peripheral benzene ring; this contrasts with the benzenoid fragment in **3** where the C3–C4, C4–C5, and C5–C6 bond lengths all are very similar. In addition, $\alpha = 53^\circ$ which is 18° larger than in **3** and of the same magnitude as in **1** [5]! Lastly, it is worth adding that **4** is not unique, other fused anionic systems such as cyclopropa(1)phenantrenyl anion [39] are structurally similar.

An important energetic parameter pertaining to the stability and possible antiaromaticity of **3** and **4** is the inversion barrier associated with their anionic centers (i.e., the energy differences between the pyramidalized and planar ions). As mentioned earlier, the calculated C_{2v} and C_s structures of **3** and **4**, respectively, are characterized as transition structures only within the DFT model. At the MP2 level these species are second-order saddle points with two imaginary frequencies. A similar thing previously was encountered

at the MP2 level for the C_{2v} structure of 7-benzocyclopropenyl anion (**1**) as this computational method predicts some puckering of the aromatic framework [5]. Despite this interesting feature of the MP2 potential energy surfaces, the calculated MP2 geometries of **3pl** and **4pl** closely resemble the corresponding transition structures located with the DFT method. Both procedures predict the planar structures to be higher in energy than their pyramidalized counterparts by similar amounts (i.e., 0.8 kcal mol⁻¹ (MP2) and 0.7 kcal mol⁻¹ (DFT) for **3** and 6.7 kcal mol⁻¹ (MP2) and 5.0 kcal mol⁻¹ (DFT) for **4**). These results reveal that the inversion barrier for **3** is smaller than for **4**, **4** has a similar barrier to **1** (4.8 kcal mol⁻¹ at the MP2 level), and the potential energy surface is shallow in both cases.

The geometries of the three-membered ring in the planar anions also are of interest. For instance, the carbon–carbon bonds emanating from the anionic center in **3pl** (C1–C11 and C10–C11) are shorter than the distal bond (C1–C10) just as in the most stable C_{2v} structure of cyclopropenyl anion [36b]. Also, the geometry of **4pl** is similar to that of **4** only the differences in the bond lengths of the small ring in the former ion are somewhat larger than in the latter (pyramidalized) species.

A few comments regarding hybridization also are warranted. 1*H*-Cyclopropa[b]naphthalene and its conjugate base have hybrid atomic orbitals whose s-characters are close to the canonical sp² value except for the atoms in the three-membered ring. As previously noted in cycloproparenes [40], the annelated bond in **3H** has a characteristic sp³–sp³ hybridization and the s-character from this bond is shifted towards the *ortho* carbon–carbon bonds (i.e., the C1 hybrid directed towards C2 has an s-content of 44.6%). This trend is amplified in **3**, where the annelated bond has very low s-character of 19.1%. The C11–H bond, on the other hand, has a very high s-content (38.3%) which is 10% larger than in **3H**. Both apical C–C bonds in the cyclopropenyl ring also have increased s-character (30.6%). These changes are in line with the practically 100% p-character of the lone pair according to the NBO analysis. In **4H** and **4** the

Table 3

NBO hybridizations, Bader's topological parameters (ρ_c , $\nabla^2\rho_c$ and ε), and Löwdin's π -bond orders, atomic charges, and π -densities for **3H**, **3**, **3pl**, **4H**, **4**, and **4pl**

Compound	Bond	NBO s-character	Bader's topological parameters			Löwdin population analysis			
			ρ_c	$\nabla^2\rho_c$	ε	π -b.o.	Atom	Charge	π -density
3H	C1–C2	44.57–34.51	0.313	–0.831	0.233	0.68	C1	–0.05	0.94
	C2–C3	34.41–33.51	0.289	–0.744	0.178	0.50	C2	–0.15	0.99
	C3–C4	33.66–34.33	0.297	–0.788	0.169	0.51	C3	0.00	0.96
	C4–C5	36.15–35.71	0.318	–0.877	0.260	0.69	C4	–0.16	0.99
	C5–C6	34.42–34.42	0.301	–0.808	0.180	0.54	C5	–0.17	0.98
	C3–C8	32.71–32.71	0.282	–0.700	0.150	0.49	C11	–0.28	1.13
	C1–C10	24.43–24.43	0.325	–0.845	0.001	0.51	H	–0.17	
	C1–C11	30.80–21.10	0.232	–0.355	0.559	0.17			
	C11–H	28.86	0.272	–0.948	0.013				
3	C1–C2	45.61–35.36	0.310	–0.808	0.309	0.66	C1	–0.03	0.88
	C2–C3	34.16–33.50	0.274	–0.673	0.186	0.41	C2	–0.31	1.22
	C3–C4	33.90–35.78	0.302	–0.795	0.218	0.58	C3	0.00	0.94
	C4–C5	35.78–35.48	0.305	–0.814	0.250	0.61	C4	–0.21	1.06
	C5–C6	35.36–35.36	0.307	–0.822	0.251	0.61	C5	–0.22	1.05
	C3–C8	32.46–32.44	0.283	–0.708	0.151	0.49	C11	–0.39	1.26
	C1–C10	19.10–19.10	0.291	–0.623	0.236	0.40	H	0.14	
	C1–C11	35.03–30.59	0.264	–0.441	0.262	0.41			
	C11–H	38.29	0.261	–0.853	0.056				
3pl	C1–C2	46.15–35.19	0.309	–0.811	0.343	0.67	C1	–0.02	0.88
	C2–C3	34.14–33.35	0.272	–0.661	0.187	0.39	C2	–0.33	1.25
	C3–C4	34.06–35.91	0.303	–0.798	0.228	0.60	C3	0.01	0.94
	C4–C5	35.72–35.36	0.303	–0.804	0.245	0.59	C4	–0.22	1.07
	C5–C6	35.51–35.51	0.309	–0.828	0.261	0.63	C5	–0.22	1.05
	C3–C8	32.47–32.47	0.283	–0.707	0.149	0.49	C11	–0.36	1.25
	C1–C10	17.91–17.91	0.283	–0.564	0.287	0.37	H	0.15	
	C1–C11	35.74–30.65	0.274	–0.475	0.133	0.46			
	C11–H	38.50	0.265	–0.905	0.057				
4H	C1–C2	42.88–32.49	0.294	–0.756	0.138	0.50	C1	–0.05	0.94
	C2–C3	35.17–34.03	0.300	–0.804	0.174	0.51	C2	0.00	0.97
	C3–C4	35.88–35.70	0.317	–0.874	0.256	0.69	C3	–0.16	0.98
	C4–C5	34.47–34.45	0.299	–0.803	0.179	0.54	C4	–0.17	0.98
	C5–C6	35.76–36.00	0.317	–0.873	0.258	0.69	C5	–0.17	0.98
	C6–C7	34.37–33.51	0.298	–0.791	0.167	0.51	C6	–0.16	0.98
	C7–C8	34.07–34.50	0.289	–0.744	0.167	0.66	C7	0.00	0.95
	C8–C9	36.21–35.83	0.312	–0.837	0.274	0.69	C8	–0.16	0.99
	C9–C10	32.80–43.05	0.294	–0.760	0.151	0.52	C9	–0.16	0.98
	C1–C10	26.50–26.44	0.342	–0.924	0.093	0.66	C10	–0.05	0.94
	C2–C7	32.19–32.30	0.284	–0.712	0.160	0.49	C11	–0.27	1.13
	C1–C11	30.34–20.68	0.227	–0.314	0.644	0.16	H	0.16	
4	C10–C11	30.24–20.89	0.228	–0.321	0.627	0.16			
	C11–H ^a	28.92 (29.41)	0.273 (0.272)	–0.952 (–0.945)	0.017 (0.016)				
	C1–C2	42.69–33.63	0.296	–0.751	0.163	0.53	C1	–0.03	0.86
	C2–C3	34.30–34.93	0.294	–0.772	0.190	0.49	C2	–0.08	1.07
	C3–C4	36.27–36.44	0.318	–0.864	0.298	0.71	C3	–0.16	0.97
	C4–C5	34.17–34.48	0.289	–0.752	0.182	0.46	C4	–0.23	1.06
	C5–C6	36.53–36.51	0.318	–0.864	0.305	0.72	C5	–0.22	1.05
	C6–C7	35.08–32.75	0.291	–0.757	0.162	0.47	C6	–0.17	1.00
	C7–C8	35.81–35.89	0.303	–0.783	0.268	0.62	C7	–0.04	1.00

Table 3 (Continued)

Compound	Bond	NBO s-character	Bader's topological parameters			Löwdin population analysis			
			ρ_c	$\nabla^2\rho_c$	ε	π -b.o.	Atom	Charge	π -density
	C8–C9	35.43–35.43	0.288	–0.724	0.240	0.51	C8	–0.22	1.08
	C9–C10	34.52–44.00	0.300	–0.759	0.222	0.59	C9	–0.27	1.14
	C1–C10	22.64–22.46	0.317	–0.782	0.089	0.56	C10	–0.04	0.86
	C2–C7	31.94–31.25	0.269	–0.643	0.144	0.38	C11	–0.45	1.29
	C1–C11	34.45–22.61	0.245	–0.383	0.314	0.36	H	0.11	
	C10–C11	33.32–20.15	0.231	–0.296	0.562	0.27			
	C11–H	23.67	0.255	–0.796	0.055				
4pl	C1–C2	43.70–32.64	0.294	–0.755	0.186	0.51	C1	–0.01	0.85
	C2–C3	35.22–35.10	0.295	–0.771	0.218	0.52	C2	–0.11	1.12
	C3–C4	36.54–36.43	0.317	–0.859	0.312	0.71	C3	–0.17	0.99
	C4–C5	33.81–34.50	0.285	–0.733	0.177	0.44	C4	–0.26	1.11
	C5–C6	36.91–36.90	0.321	–0.873	0.327	0.75	C5	–0.21	1.05
	C6–C7	34.82–32.07	0.284	–0.728	0.143	0.43	C6	–0.18	1.00
	C7–C8	37.12–36.78	0.310	–0.801	0.335	0.69	C7	–0.04	1.01
	C8–C9	34.37–34.66	0.270	–0.651	0.203	0.39	C8	–0.03	1.12
	C9–C10	34.73–46.54	0.307	–0.788	0.350	0.69	C9	–0.03	1.21
	C1–C10	20.50–20.21	0.300	–0.673	0.148	0.47	C10	–0.03	0.89
	C2–C7	32.02–30.69	0.262	–0.618	0.142	0.34	C11	–0.38	1.28
	C1–C11	35.64–32.08	0.281	–0.515	0.234	0.53	H	0.15	
	C10–C11	33.05–27.97	0.246	–0.326	0.425	0.28			
	C11–H	39.76	0.265	–0.904	0.068				

^a The C–H bonds of the methylene group are not equivalent. Parenthetical values correspond to the longer (1.093 Å vs. 1.092 Å) bond.

three-membered rings retain the characteristics of the linear isomers, but the low s-content of the annelated bonds in the former species are counteracted by relatively high π -electron densities concentrated in this bond as reflected by their π -bond orders (0.66, **4H** and 0.56, **4**). The contradictory effects of rehybridization and the π -electron distribution in the angularly fused anion are consistent with its higher energy content. In addition, $\alpha = 53.6^\circ$, which implies that the apical C–C bonds in the cyclopropenyl fragment are more twisted than in **3** [41]. The resonance structures shown in Scheme 2 also suggest that the π -bond order of the C1–C10 bond in **4** is diminished and that the C1–C11 π -bond order is larger than for the C10–C11 bond, which is exactly what is observed.

Pronounced differences in the electronic structures of **3** and **4** also are reflected in the Laplacian ($\nabla^2\rho_c$) and ellipticity (ε) values derived from a topological analysis of the electron density distribution (Table 3). For instance, there is a significant decrease in $\nabla^2\rho_c$ (–0.623 vs. –0.782) for the fused bond on going

from **3** to **4**. There also is a change in the electron density (ρ_c) in the same direction, but to a smaller extent (0.291 vs. 0.317). Similarly, the ellipticity (a measure of the anisotropy of the charge distribution) of this bond decreases upon going from **3** (0.236) to **4** (0.089) as expected due to the smaller π -bond character in the latter case. As for the apical bonds, opposite effects are noted; the Laplacian increases, and the ellipticity also undergoes a pronounced change, increasing from 0.262 to 0.314 and 0.562. These parameters indicate again that there is considerably stronger conjugation in the aromatic π -system of **3**. Finally, the linear isomer also has a slightly larger density at the three-membered ring critical point (0.228, **3** vs. 0.213, **4**) which is indicative of greater surface delocalization.

3.3. Electron affinity calculations

The relative stabilities of **3** and **4** can be probed further by computing the electron affinities of their

Table 4
Computed DFT electron affinities and bond dissociation energies

Compound	EA			Compound	BDE		
	Direct	Isogyric reaction ^a	Experiment		Direct	Isogyric reaction ^a	Experiment
1r	1.067	0.795	0.8 ± 0.3 ^b	1H	98.3	89.9	90.8 ± 7.5 ^b
2r	1.184		0.912 ± 0.006 ^c	2H	98.2		89.8 ± 0.6 ^c
3r	1.642	1.370		3H	94.5	86.1	
4r	1.167	0.895		4H	99.1	90.7	

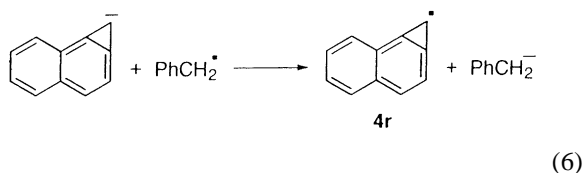
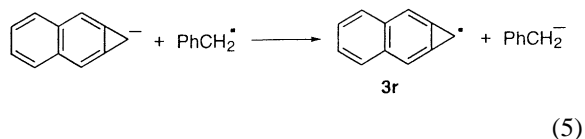
Electron affinities (0 K) in electron volts and bond dissociation energies (298 K) in kilocalories per mole.

^a Calculated vs. benzyl radical.

^b [5].

^c [42].

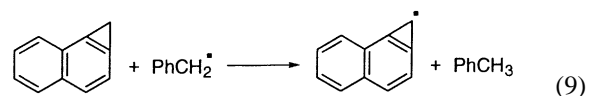
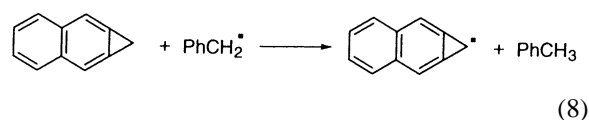
corresponding radicals (**3r** and **4r**, respectively). To this end, we calculated these quantities and the EA of 7-benzocyclopropenyl radical (**1r**) using the BVWN5/6-31+G(d) method. This approach has been shown to give reasonable results for a few compounds, but since the number of substrates that were examined is small and the absolute values are approximately 8 kcal mol⁻¹ too large, isogyric reactions were employed Eqs. (5) and (6) [36b]. To obtain the EAs of **3r** and **4r**, the experimental value for benzyl radical was used as indicated in Eq. (7) [42], and the results are summarized in Table 4.



$$\text{EA}(\mathbf{3r} \text{ or } \mathbf{4r}) = \Delta H^\circ(\text{Eq. 5 or 6}) + \text{EA}(\text{PhCH}_2^\bullet)_{\text{expt}} \quad (7)$$

In keeping with the work of Merrill and Kass [36b], the directly computed BVWN5 electron affinity of benzyl radical is too large by 6.3 kcal mol⁻¹ but the error is systematic and the calculated value for 7-benzocyclopropenyl radical (**1r**) via an isogyric reaction analogous to Eq. (5) is in excellent agreement

with experiment. Thus, we predict that the electron affinities of **3r** and **4r** are 1.37 and 0.90 eV, respectively. As the latter value is the smaller of the two, this provides additional evidence that the linear anion **3** is more stable than its angular (**4**) counterpart. In a similar manner, the C11–H bond dissociation energies of **3H** and **4H** were computed via isogyric reactions 8 and 9.



The results also are summarized in Table 4 and the BDEs for both compounds are about the same as for toluene (89.8 ± 0.6 kcal mol⁻¹) [42] and benzocyclobutene (92 ± 4 kcal mol⁻¹) [22].

As for the antiaromaticity of **3** and **4**, this can be addressed by comparing the acidities of their conjugate acids with 1-methylnaphthalene and 2-methylnaphthalene. 1H-Cyclopropa[b]naphthalene (**3H**) is 7.6 ± 3.0 kcal mol⁻¹ more acidic than its acyclic analog (i.e., 2-methylnaphthalene). On the other hand, **4H** is predicted to be almost 10 kcal mol⁻¹ less acidic than either of the two methylnaphthalenes. This latter ordering is the same as for benzocyclopropene/toluene and benzocyclobutene/toluene (experimentally the cyclic compound is less acidic by 4 ± 3 kcal mol⁻¹ in both cases [5,22] whereas computationally the

difference is $\sim 2 \text{ kcal mol}^{-1}$), but the difference between **4H** and **5H** or **6H** is significantly greater. These acidity orderings are directly related to the ability of the aromatic ring to delocalize the charge and in the case of the annelated three-membered ring compounds, to alleviate unfavorable cyclopropenyl anion-like 4π -electron interactions. These depend on the size of the aromatic system and the bond localization pattern inherent to the aromatic moiety. Given the data above, one can conclude that **3** is an aromatic ion whereas **4** is antiaromatic based upon the energetic criterion of aromaticity and antiaromaticity [35].

4. Conclusions

The conjugate bases of 1*H*-cyclopropa[b]naphthalene and 2-methylnaphthalene were generated in a FTMS by proton abstraction of their corresponding hydrocarbons with fluoride ion. Equilibrium constants with several standard reference acids were measured and the resulting acidities are as follows: $\Delta G_{\text{acid}}^{\circ}(\mathbf{3H}) = 357.5 \pm 2.1 \text{ kcal mol}^{-1}$, $\Delta H_{\text{acid}}^{\circ}(\mathbf{3H}) = 365.1 \pm 2.1 \text{ kcal mol}^{-1}$, $\Delta G_{\text{acid}}^{\circ}(\mathbf{6H}) = 365.2 \pm 2.1 \text{ kcal mol}^{-1}$, and $\Delta H_{\text{acid}}^{\circ}(\mathbf{6H}) = 372.7 \pm 2.1 \text{ kcal mol}^{-1}$. The measured acidities show that **3H** is $7.6 \pm 3.0 \text{ kcal mol}^{-1}$ more acidic than **6H**, in contrast to the acidity ordering for benzocyclopropene and toluene. These experimental findings are satisfactorily reproduced by ab initio and DFT calculations carried out at the MP2/6-31+G(d)/MP2/6-31G(d) and

BWVN5/6-31+G(d) levels. As for the origin of this reversal, it is rationalized by an increase in the aromatic ring size and a diminishment of the importance of the 4π -electron interaction in the annelated cyclopropenyl anion. Consequently, **3** can be viewed as an aromatic ion. In contrast, **4** is $\sim 10 \text{ kcal mol}^{-1}$ less stable than its acyclic counterparts and has a harder time alleviating the unfavorable 4π -electron interaction in the three-membered ring. It is best viewed as an antiaromatic ion.

Acknowledgements

Support from the National Science Foundation, the donors of the Petroleum Research Foundation, as administered by the American Chemical Society, the Minnesota Supercomputer Institute, and the University of Minnesota-IBM Shared Research Project are gratefully acknowledged. The work in Zagreb (I.A., Z.G., and M.E.M.) has been supported by the Ministry of Science and Technology of Croatia through project 00980801 and HR-US project JF 143.

Appendix A

MP2/6-31G(d) and BVWN5/6-31+G(d) structures for 1-methylnaphthalene (**5H**), 1-methylnaphthalenyl anion (**5**), 2-methylnaphthalene (**6H**) and 2-methylnaphthalenyl anion (**6**). All distances are in angstroms and angles in degrees.

Bond or angle	5H		5	
	MP2/6-31G(d)	BVWN5/6-31+G(d)	MP2/6-31(G)(d)	BVWN5/6-31+G(d)
C1–C2	1.430	1.447	1.478	1.499
C2–C3	1.420	1.434	1.410	1.419
C3–C4	1.381	1.391	1.390	1.406

Appendix A (Continued)

Bond or angle	5H		5	
	MP2/6-31G(d)	BVWN5/6-31+G(d)	MP2/6-31(G)(d)	BVWN5/6-31+G(d)
C4–C5	1.412	1.425	1.408	1.421
C5–C6	1.379	1.389	1.383	1.394
C6–C7	1.418	1.432	1.424	1.440
C7–C8	1.418	1.432	1.411	1.426
C8–C9	1.377	1.387	1.399	1.415
C9–C10	1.413	1.426	1.386	1.396
C10–C1	1.384	1.395	1.441	1.455
C2–C7	1.434	1.452	1.445	1.464
C1–C11	1.506	1.526	1.377	1.397
C10–C1–C11	120.4	120.0	122.3	121.0
C10–C1–C2	118.9	118.8	113.8	114.9
C1–C2–C3	122.3	122.8	121.1	122.0
C2–C3–C4	121.0	121.4	122.7	123.1
C3–C4–C5	120.5	120.4	119.3	119.1
C4–C5–C6	119.9	119.8	119.5	119.7
C5–C6–C7	120.9	121.2	122.6	122.4
C6–C7–C8	121.2	121.4	121.6	121.6
C7–C8–C9	120.3	120.4	118.2	118.8
C8–C9–C10	120.2	120.2	122.6	122.3
C9–C10–C1	121.7	121.9	122.6	123.1
C1–C2–C7	119.4	119.2	120.5	120.3
C7–C2–C3	118.2	117.9	118.1	117.7
C6–C7–C2	119.3	119.2	117.6	117.8
C2–C7–C8	119.4	119.4	120.5	120.6
	6H		6	
C1–C2	1.382	1.393	1.436	1.450
C2–C3	1.419	1.433	1.396	1.409
C3–C4	1.419	1.432	1.433	1.451
C4–C5	1.380	1.391	1.383	1.393
C5–C6	1.414	1.427	1.414	1.428

Appendix A (Continued)

Bond or angle	6H		6	
	MP2/6-31G(d)	BVWN5/6-31+G(d)	MP2/6-31(G)(d)	BVWN5/6-31+G(d)
C6–C7	1.380	1.391	1.390	1.407
C7–C8	1.418	1.432	1.406	1.417
C8–C9	1.419	1.432	1.428	1.444
C9–C10	1.378	1.388	1.369	1.378
C10–C1	1.420	1.435	1.455	1.469
C3–C8	1.431	1.448	1.448	1.468
C1–C11	1.506	1.526	1.379	1.401
C10–C1–C11	119.7	119.9	120.7	120.8
C10–C1–C2	118.7	118.3	113.7	114.2
C1–C2–C3	121.6	122.0	123.4	123.6
C2–C3–C4	122.0	122.4	123.3	123.5
C3–C4–C5	120.7	120.9	122.2	121.9
C4–C5–C6	120.3	120.3	120.9	121.2
C5–C6–C7	120.3	120.2	118.5	118.5
C6–C7–C8	120.6	120.9	121.7	122.0
C7–C8–C9	122.3	122.8	122.9	123.3
C8–C9–C10	120.7	121.1	121.7	122.1
C9–C10–C1	121.3	121.4	123.6	123.2
C2–C3–C8	119.1	118.9	120.6	120.2
C8–C3–C4	118.9	118.7	115.9	116.3
C7–C8–C3	119.1	119.0	120.4	120.1
C3–C8–C9	118.5	118.2	116.5	116.6

References

- [1] C. Eaborn, R. Eidenschink, S.J. Harris, D.R.M. Walton, J. Organomet. Chem. 124 (1977) C27–C29.
- [2] (a) B. Halton, C.J. Randall, J.P. Stang, J. Am. Chem. Soc. 106 (1984) 6108;
 (b) B. Halton, C.J. Randall, G.J. Gainsford, J.P. Stang, J. Am. Chem. Soc. 108 (1986) 5949;
 (c) B. Halton, S.J. Buckland, Q. Lu, Q. Mei, J.P. Stang, J. Org. Chem. 53 (1988) 2418.
- [3] B. Halton, J.P. Stang, Synlett. 2 (1997) 145.
- [4] B. Halton, Q. Lu, W.H. Melhuish, J. Photochem. Photobiol. A: Chem. 52 (1990) 205.
- [5] L. Moore, R. Lubinski, M.C. Baschky, G.D. Dahlke, M. Hare, T. Arrowood, Z. Glasovac, M. Eckert-Maksic, S.R. Kass, J. Org. Chem. 62 (1997) 7390.
- [6] 7-Methylbenzocyclopropenyl anion has been suggested previously as a fragment ion in the collision-induced dissociation spectrum of the parent ion of a benzocyclopentanedione. See: J.H. Bowie, T. Blumenthal, M.H. Laffer, S. Janposri, G.E. Gream, Aust. J. Chem. 37 (1984) 1447.
- [7] C. Eaborn, D.R.M. Walton, G. Seconi, Chem. Commun. (1975) 937.
- [8] (a) P. Müller, Carbocyclic ring compounds, in: A. de Meijere (Ed.), Houben-Weyl Methoden Organischen Chemie, vol. E/17d, Thieme, Stuttgart, 1997;

- (b) P. Müller, Advances in theoretically interesting molecules, in: R.P. Thummel (Ed.), vol. 3, JAI Press, Greenwich, CT, 1995, p. 37;
- (c) B. Halton, The chemistry of the cyclopropyl group, in: Z. Rappoport (Ed.), vol. 2, Wiley, New York, 1995.
- [9] A.R. Browne, B. Halton, C.W. Spangler, *Tetrahedron* 30 (1974) 3289.
- [10] P. Müller, G. Bernardinelli, H.C.G.-N. Thi, *Helv. Chim. Acta* 72 (1989) 1627.
- [11] (a) K.M. Broadus, S. Han, S.R. Kass, *J. Org. Chem.* 66 (2001) 99;
- (b) T.L. Arrowood, S.R. Kass, *J. Am. Chem. Soc.* 121 (1999) 7272;
- (c) S. Han, S.R. Kass, *J. Chem. Soc. Perkin Trans. 1* (1999) 1553;
- (d) H.G. Koser, G.E. Renzoni, W.T. Borden, *J. Am. Chem. Soc.* 105 (1983) 6360;
- (e) R. Breslow, *Pure Appl. Chem.* 54 (1982) 927;
- (f) M.R. Wasielewski, R. Breslow, *J. Am. Chem. Soc.* 98 (1976) 4222;
- (g) R. Breslow, *Acc. Chem. Research* 6 (1973) 393;
- (h) R. Breslow, *Angew. Chem. Int. Ed. Engl.* 7 (1968) 565;
- (i) R. Breslow, J. Brown, J.J. Gajewski, *J. Am. Chem. Soc.* 89 (1967) 4383;
- (j) R. Breslow, *Chem. Eng. News* 43 (1965) 90.
- [12] (a) J.E. Bartmess, S.S. Griffith, *J. Am. Chem. Soc.* 112 (1990) 2931;
- (b) M. Meot-Ner, J.F. Liebman, S.A. Kafafi, *J. Am. Chem. Soc.* 110 (1988) 5937.
- [13] T.C.L. Wang, T.L. Ricca, A.G. Marshall, *Anal. Chem.* 58 (1986) 2935.
- [14] A.G. Marshall, D.C. Roe, *J. Chem. Phys.* 73 (1980) 1581.
- [15] K.M. Broadus, S.R. Kass, *J. Chem. Soc. Perkin Trans. 2* (1999) 2389.
- [16] M.J. Frisch, G.W. Trucks, H.B. Schlegel, P.M.W. Gill, B.G. Johnson, M.A. Robb, J.R. Cheeseman, T. Keith, G.A. Peterson, J.A. Montgomery, K. Raghavachari, M.A. Al-Laham, V.G. Zakrewski, J.V. Ortiz, J.B. Foresman, J. Cioslowski, B.B. Stefanov, A. Nanayakkara, M. Challacombe, C.Y. Peng, R.Y. Ayala, W. Chen, M.W. Wong, J.L. Andres, E.S. Replogle, R. Gomperts, R.L. Martin, D.J. Fox, J.S. Binkley, D.J. Defrees, J. Baker, J.P. Stewart, M. Head-Gordon, C. Gonzalez, J.A. Pople, Gaussian 94, Gaussian Inc., Pittsburgh, PA, 1995.
- [17] M.J. Frisch, G.W. Trucks, H.B. Schlegel, G.E. Scuseria, M.A. Robb, J.R. Cheeseman, V.G. Zakrzewski, J.A. Montgomery Jr., R.E. Stratmann, J.C. Burant, S. Dapprich, J.M. Millam, A.D. Daniels, K.N. Kudin, M.C. Strain, O. Farkas, J. Tomasi, V. Barone, M. Cossi, R. Cammi, B. Mennucci, C. Pomelli, C. Adamo, S. Clifford, J. Ochterski, G.A. Petersson, P.Y. Ayala, Q. Cui, K. Morokuma, D.K. Malick, A.D. Rabuck, K. Raghavachari, J.B. Foresman, J. Cioslowski, J.V. Ortiz, A.G. Baboul, B.B. Stefanov, G. Liu, A. Liashenko, P. Piskorz, I. Komaromi, R. Gomperts, R.L. Martin, D.J. Fox, T. Keith, M.A. Al-Laham, C.Y. Peng, A. Nanayakkara, M. Challacombe, P.M.W. Gill, B. Johnson, W. Chen, M.W. Wong, J.L. Andres, C. Gonzalez, M. Head-Gordon, E.S. Replogle, J.A. Pople, Gaussian 98, Gaussian, Inc., Pittsburgh PA 1998.
- [18] GAMESS, M.W. Schmidt, K.K. Baldrige, J.A. Boatz, S.T. Elbert, M.S. Gordon, J.H. Jensen, S. Koseki, N. Matsunaga, K.A. Nguyen, S.J. Su, T.L. Windus, M. Dupuis, J.A. Montgomery, *J. Comp. Chem.* 14 (1993) 1347.
- [19] J.A. Pople, R. Seeger, R. Krishnan, *Int. J. Quant. Chem. Symp.* 11 (1977) 149.
- [20] W.J. Hehre, L. Radom, P.v.R. Schleyer, J.A. Pople, *Ab Initio Molecular Orbital Theory*, Wiley, New York, 1986.
- [21] Z.B. Maksic, M. Eckert-Maksic, M. Hodoscek, W. Koch, D. Kovacek, Theoretical studies of the Mills–Nixon effect in molecules in natural science and medicine, in: Z.B. Maksic, M. Eckert-Maksic (Eds.), *An Encomium for Linus Pauling*, Ellis Horwood, Chichester, 1991, p. 333.
- [22] Z. Glasovac, M. Eckert-Maksic, K.M. Broadus, M.C. Hare, S.R. Kass, *J. Org. Chem.* 65 (2000) 1818.
- [23] (a) A.D. Becke, *Phys. Rev. A: Gen. Phys.* 38 (1988) 3098;
- (b) S.H. Vosko, L. Wilk, M. Nusair, *Can. J. Phys.* 58 (1980) 1200.
- [24] A.P. Scott, L. Radom, *J. Phys. Chem.* 100 (1996) 16502.
- [25] (a) Z.B. Maksic, in: Z.B. Maksic (Ed.), *Theoretical Models of Chemical Bonding*, vol. 2, Springer Verlag, Berlin-Heidelberg, 1991, p. 137;
- (b) L. Pauling, *J. Am. Chem. Soc.* 53 (1931) 1367.
- [26] R. McWeeny, *Coulson's Valence*, 3rd ed., Oxford University Press, Oxford, 1979.
- [27] (a) A.E. Reed, F. Weinhold, *J. Phys. Chem.* 78 (1983) 1736;
- (b) A.E. Reed, L.A. Curtiss, F. Weinhold, *Chem. Rev.* 88 (1988) 899.
- [28] (a) E.D. Glendening, A.E. Reed, J.E. Carpenter, F. Weinhold, *NBO*, Version 3.1.
- [29] P.O. Löwdin, *J. Chem. Phys.* 18 (1950) 365.
- [30] (a) R.F.W. Bader, *Atoms in Molecules: A Quantum Theory*, Oxford University Press, Oxford, 1990;
- (b) The implementation in Gaussian 94 is due to Cioslowski and coworkers. See: J. Cioslowski, A. Nanayakkara, M. Challacombe, *Chem. Phys. Lett.* 203 (1993) 137 and the Gaussian 94 manual for more details.
- [31] All thermodynamic data, unless otherwise noted, come from S.G. Lias, J.E. Bartmess, J.F. Liebman, J.L. Holmes, R.D. Levin, W.G. Mallard, *J. Phys. Chem. Ref. Data* 17 (1988) Suppl. 1 [or the slightly updated from available on a personal computer, NIST Negative Ion Energetics Database (Version 3.00, 1993); NIST Standard Reference Database 19B.] or [32].
- [32] J.E. Bartmess, *Negative Ion Energetics Data in Secondary Negative Ion Energetic Data*, 1998, National Institute of Standards and Technology, Gaithersburg, MD 20899 <http://webbook.nist.gov>.
- [33] The calculated structures of **1H** and **1** are very similar to their MP2/6-31+G* geometries reported in [5].
- [34] (a) E. Clar, *The Aromatic Sextet*, Wiley, New York, 1972;
- (b) E. Clar, R. Schoental, *Polycyclic Hydrocarbons*, vols. 1 and 2, Academic Press and Springer Verlag, 1964.

- [35] (a) V.I. Minkin, M.N. Glukhovtsev, B.Y. Simkin, *Aromaticity and Antiaromaticity. Electronic and Structural Aspects*, Wiley, New York, 1994;
(b) P.J. Garratt, *Aromaticity*, Wiley, New York, 1986.
- [36] (a) S. Han, M.C. Hare, S.R. Kass, *Int. J. Mass Spectrom. Ion Proc.* 201 (2000) 101;
(b) G.N. Merrill, S.R. Kass, *J. Am. Chem. Soc.* 119 (1997) 12322;
(c) M.N. Glukhovtsev, S. Laiter, A. Pross, *J. Phys. Chem.* 100 (1996) 17801;
(d) P.v.R. Schleyer, E. Kaufmann, G.W. Spitznagel, R. Janoschek, G. Winkelhofer, *Organometallics* 5 (1986) 79;
(e) G. Winkelhofer, R. Janoschek, F. Fratev, G.W. Spitznagel, J. Chandrasekhar, P.v.R. Schleyer, *J. Am. Chem. Soc.* 107 (1985) 332.
- [37] (a) M. Eckert-Maksic, Z.B. Maksic, M. Hodoscek, K. Poljanec, *Int. J. Quant. Chem.* 42 (1992) 869;
(b) Z.B. Maksic, M. Eckert-Maksic, D. Kovacek, D. Margetic, *J. Mol. Struct. (Theochem.)* 260 (1992) 241;
(c) M. Eckert-Maksic, Z. Glasovac, Z.B. Maksic, I. Zrinski, *J. Mol. Struct. (Theochem.)* 366 (1996) 173.
- [38] (a) O. Mó, M. Yáñez, M. Eckert-Maksic, Z.B. Maksic, *J. Org. Chem.* 60 (1995) 1638;
(b) W. Koch, M. Eckert-Maksic, Z.B. Maksic, *J. Chem. Soc. Perkin Trans. 2* (1993) 2195;
(c) Z.B. Maksic, M. Eckert-Maksic, K.-H. Pfeifer, *J. Mol. Struct. (Theochem.)* 300 (1993) 445.
- [39] M. Eckert-Maksic, Z. Glasovac, N. Novak-Coumbassa, in preparation.
- [40] (a) J.A. Pople, B.T. Luke, M.J. Frisch, J.S. Binkley, *J. Phys. Chem.* 89 (1985) 2198;
(b) J.A. Pople, L.A. Curtiss, *J. Phys. Chem.* 91 (1987) 367;
(c) L.A. Curtiss, J.A. Pople, *J. Phys. Chem.* 92 (1988) 894;
(d) C.A. Deakyne, J.F. Liebman, in: P.v.R. Schleyer (Ed.), *Encyclopedia of Computational Chemistry*, vol. 2, Wiley, Chichester, 1997, p. 1439.
- [41] Z.B. Maksic, L. Klasinc, M. Randic, *Theoret. Chim. Acta* 4 (1966) 273.
- [42] G.B. Ellison, G.E. Davico, V.M. Bierbaum, C.H. DePuy, *Int. J. Mass Spectrom. Ion Processes* 156 (1996) 109.